Research Article
Research on High Frequency Model of Hybrid Vehicle Battery

Yang Yongming, Yao Mo and Wang Quandi
School of Electrical Engineering, Chongqing University, Chongqing, 400044, China

Abstract: The application of motor and converter in hybrid vehicle can lead to a significant increase in electromagnetic compatibility. The influence of traction batteries as part of the electromagnetic interference path was not well considered. In this study, high frequency circuit models of single cell, cells connected in series and cells connected in parallel were proposed and developed based on their impedance characteristics and their structure features. Finally, values calculated based on the models and dates measured actually were compared and analyzed. The results show the calculation high frequency losses and the simulation as interference path.

Keywords: Batteries, EMC, hybrid vehicles, impedance, modeling

INTRODUCTION

With resources and environment problems being increasingly serious, hybrid cars are rapidly developed by Madi *et al.* (2008). However, the battery pack, as one of the hybrid cars power source, is directly connected to the DC/AC inverter to provide energy to the drive motor, which makes high frequency harmonic interference signals produced by the power switching device transmitted though the battery pack and then produce electromagnetic compatibility problems by Ehsani *et al.* (2007) and Mutoh *et al.* (2005), similar work by Omar *et al.* (2012). So study the frequency characteristic of the power battery, set the high frequency model of battery is of great significance to electromagnetic interference suppression and system modeling and simulation of electromagnetic interference.

MATERIALS AND METHODS

For the power batteries, when the frequency is higher than 1kHz, polarization effect of the battery on its impedance characteristics is very small, while the skin effect of the battery electrode and the connecting wire make a big difference. The impedance of battery electrolyte plays a decisive role in the battery impedance characteristics by Chen *et al.* (2006) and Aesic and Wei (2011), similar work by Zhang *et al.* (2010). The electrode impedance mainly functions as the resistance and inductance of the electrode and the capacitance polarization effect is so small that the impedance of the electrolyte can be treated as a resistance.
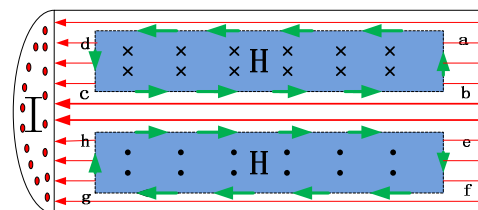

Fig. 1: A conductor internal electromagnetic induction

For batteries' high-frequency modeling, the actually porous electrode was taken as cylindrical electrode and due to the skin effect the calculation method of high-frequency resistance differs from DC resistance.

At low frequencies, the current density distribution inside the conductor is uniform. From the conductor cross-section, current flow is the same in the center and the edge area. While at high frequencies, current density of conductor surface becomes large and there is almost no current flow in the center regional. It is called the skin effect that the low frequency current evenly fill the entire wire while high frequency current only flows through the surface region of the conductor.

When a high frequency current flow into a cylindrical conductor, longitudinal section of cylindrical conductor as shown in Fig. 1, it will generate a changing magnetic field inside the conductor. If a current direction is horizontal to the left, it will generate a magnetic field as is shown in the internal conductor, Induction electromotive force will be produced in the planar *abcd* and *efgh*. This Induction EMF will cause eddy currents in the conductor to prevent the change of flux. Inside the conductor the direction of eddy *cb* and *he* is opposite to the main

Corresponding Author: Yang Yongming, School of Electrical Engineering, Chongqing University, Chongqing, 400044, China
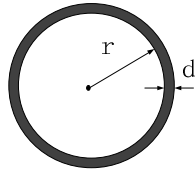
Fig. 2: Skin impedance diagram

current, which weakens the current, while, in the surface of the conductor the direction of vortex *ad* and *fg* is the same with the main current, the current was strengthen. As a result current tends to flow through from the surface of the conductor.

For the high-frequency circuit, the change rate of current is very huge, the phenomenon of uneven distribution will be more serious. The maximum EMF was induced in the center area of the conductor by the magnetic field generated by the high-frequency current in the conductor. Since the induction electromotive force generates an induction current in the closed circuit, the maximum induced current appears in the center of the conductor, which is contrary to the direction of the primary current, as a result it force the current close to the outer surface of the conductor. Thus, the internal conductor is actually no current and current is concentrated in a thin layer adjacent to the wire outer. Results in the increase of its impedance value. Therefore, calculating the high-frequency impedance of the conductor skin effect must be considered, as is shown in Fig. 2 cylindrical electrode resistance is calculated:

From the basic formula of conductor resistance:

$$R = \frac{l}{\gamma \cdot S} \tag{1}$$

where,
l = The length of the conductor
S = The cross-sectional area of the conductor
y = The conductivity of the conductor

When high frequency current is applied, the current is concentrated in a thin layer of the outer conductor surface, the effective cross-sectional area $S = 2\pi r \cdot d$ .where d is the penetration depth $d = \sqrt{\frac{2}{2\pi f \mu \gamma}}$, (μis the permeability of the electrode).Thus under the effect of high frequency current the resistance of cylindrical conductor electrode is as follows:

$$R_{ac}(f) = \sqrt{\frac{\mu}{4\pi r^2 \gamma} \cdot f} \cdot l \tag{2}$$

Inductance generated by the current carrying electrodes which are composed of two parts: one part is the internal inductance L',which is generated by the magnetic flux inside the conductor that linked only parts of the conductor, the other part is the external
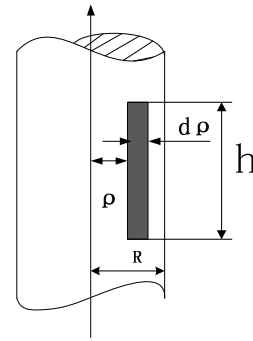

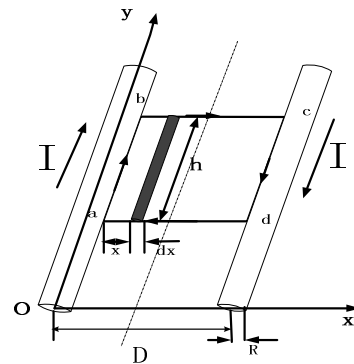Fig. 3: Internal inductance calculation diagram

Fig. 4: External inductance calculation diagram

inductance L'', which is generated by flux that linked the entire conductor current:

$$L = L' + L'' \tag{3}$$

As Fig. 3 shows, the internal inductance:
When $\rho \le R$:

$$B = \frac{\mu_0 I'}{2\pi\rho} = \frac{\mu_0}{2\pi\rho} \frac{I}{\pi R^2} \pi\rho^2 = \frac{\mu_0 I\rho}{2\pi R^2} \tag{4}$$

internal flux of the electrode:

$$d\psi' = \frac{I'}{I} d\Phi = \frac{\rho^2}{R^2} d\Phi = \frac{\mu_0 Ih}{2\pi R^4} \rho^3 d\rho \tag{5}$$

$$\psi' = \frac{\mu_0 Ih}{2\pi R^4} \int_0^R \rho^3 d\rho = \frac{\mu_0 Ih}{8\pi} \tag{6}$$

The internal inductance of one electrode:

$$L' = \frac{\psi'}{I} = \frac{\mu_0 h}{8\pi} \tag{7}$$

The external inductance is shown in Fig. 4.

The magnetic vector potential generated by those two electrodes: $A = \frac{\mu_0 I}{2\pi} \ln \frac{r_1}{r_2}$, where r_1, r_2 denotes the distance between the field point and the positive current, the negative current.

External magnetic flux of the two electrodes:

$$\psi'' = \Phi = \oint_l A \bullet dl$$
$$= \frac{\mu_0 I}{2\pi} \left(\int_{ab} \ln \frac{D-R}{R} dl + \int_{cd} \ln \frac{D-R}{R} dl \right) \quad (8)$$
$$= \frac{\mu_0 I h}{\pi} \ln \frac{D-R}{R}$$

The external inductance of the two electrodes:

$$L'' = \frac{\psi''}{I} = \frac{\mu_0 h}{\pi} \ln \frac{D-R}{R} \quad (9)$$

The electrode inductance:

$$L = L' + L'' = \frac{\mu_0 h}{8\pi} \times 2 + \frac{\mu_0}{\pi} \ln \frac{D-R}{R}$$
$$= \frac{\mu_0 h}{4\pi} + \frac{\mu_0}{\pi} \ln \frac{D-R}{R} \quad (10)$$

where,
D = The distance between the two electrodes
R = The electrode equivalent radius

When frequencies higher than 1kHz, the polarization effect of the battery is not obvious, the equivalent impedance of the electrolyte within the battery can be equivalent to R_0. Therefore, the high frequency equivalent model of the battery can be modeled as shown in Fig. 5.

The complex impedance is measured with the Agilent impedance analyzer 4294A and its standards measurements fixture 16047E, shown in Fig. 6.

To get the measurement impedance value of the battery, the impedance of block condenser must be removed from the total measurement result. The computation process of battery impedance is derived as follows:

$$Z_{total} = Z_{bat} + Z_{cap} = \text{Re}(Z_{total}) + j\,\text{Im}(Z_{total}) \quad (11)$$

$$Z_{cap} = \text{Re}(Z_{cap}) + j\,\text{Im}(Z_{cap}) \quad (12)$$

$$Z_{bat} = Z_{total} - Z_{cap}$$
$$= \text{Re}(Z_{total}) - \text{Re}(Z_{cap}) + j[\text{Im}(Z_{total}) - \text{Im}(Z_{cap})]$$
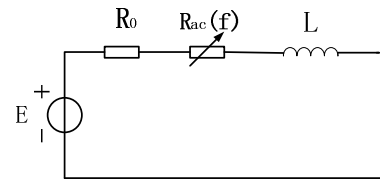$$= \text{Re}(Z_{bat}) + j[\text{Im}(Z_{bat})] \quad (13)$$

Fig. 5: High frequency equivalent model of the battery

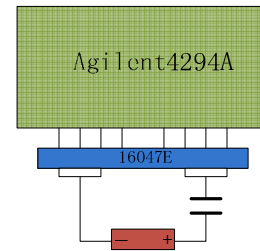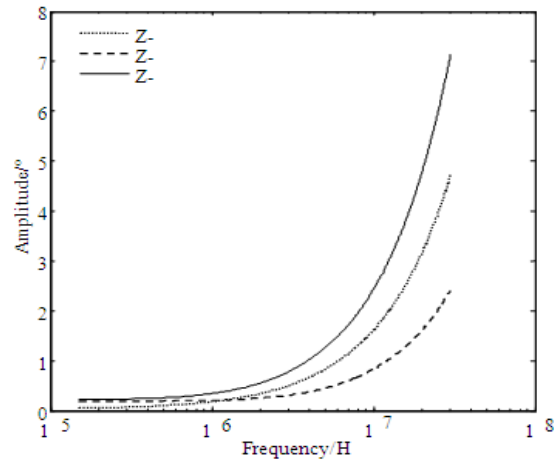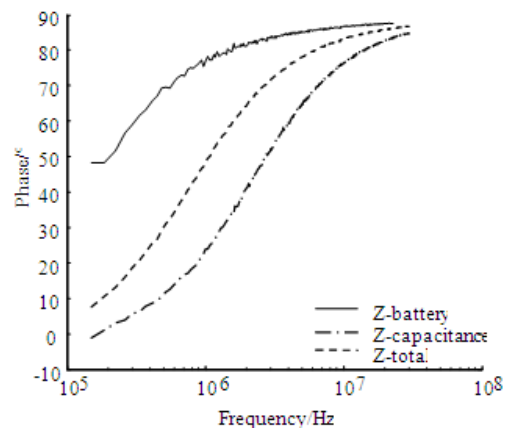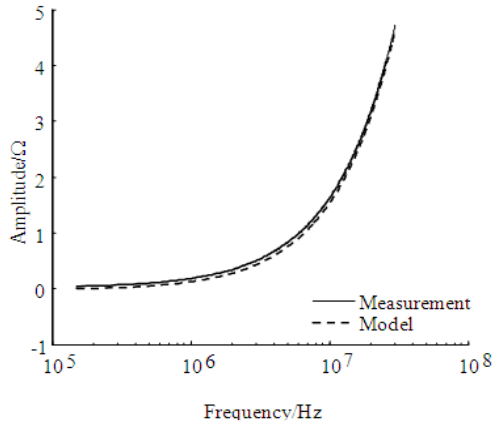Fig. 6: Masurement methods
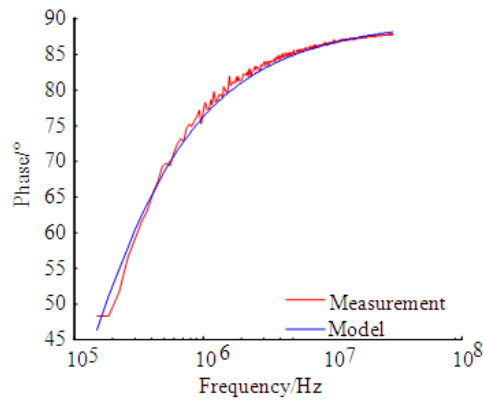

(a) Amplitude-frequency

(b) Phase-frequency

Fig. 7: The impedance calculation results of the single cell

The value of measurement and model for cell is shown in Fig. 7, compare the measured impedance

(a) Amplitude-frequency

(a) Amplitude-frequency

(b) Phase-frequency

(b) Phase-frequency

Fig. 8: Comparison of measured and simulated impedance curves for a cell

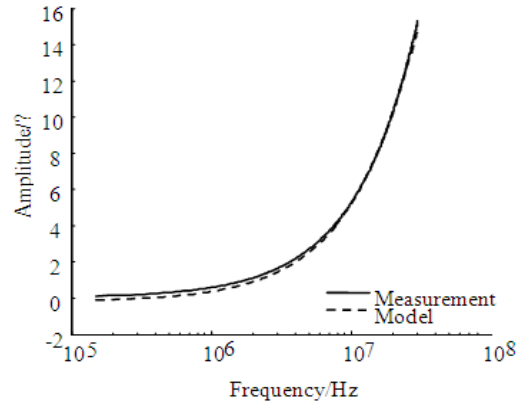Fig. 9: Comparison of measured and simulated impedance curves for cells in series

curve and the calculated impedance curve and then analyze the causes of the error. Because the power battery is not used alone in the practical application and generally used on multiple cells in series to raise the output voltage, multiple cells in parallel to increase the output power, the high frequency characteristics of cells connected in series and in parallel were also analyzed in this study.

The comparison of the measured impedance curve and the calculated impedance curve is shown in Fig. 8.
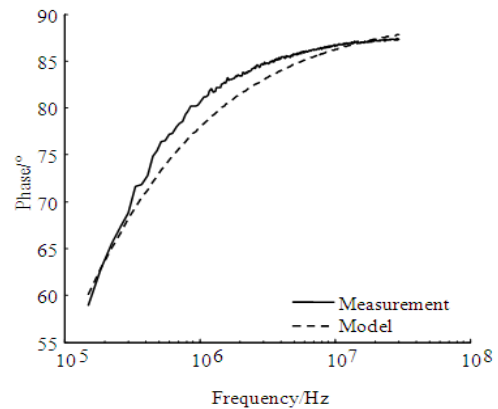
Take four cells connected in series for example. The impedance of four cells in series is about four times the value of single battery cell, however, the connection between the battery cells will produce a parasitic capacitance effection and the connecting wires between the batteries will affect their impedance values, taking those into account the calculation results also need to be corrected.

The model parameters of battery in series:

$$R_{series} = 4 \times (R_0 + R_{ac}(f)) - k_1, \quad L_{series} = 4 \times L - k_2$$

where $k_1 = 0.046$ is the correction factor for the resistance value of batteries in series, $k_2 = 1.865 \times 10^{-8}$ is the correction factor for the inductance value. Figure 9 shows the comparison of the measured impedance value and the calculated impedance value.

The agreement between measured and simulated value of the impedance shows the suitability of the proposed conducted EMI model for the series battery, which illustrates that the high frequency model of series battery can be correctly derived through the model of the battery cell.

The connection of cells in parallel is shown in Fig. 10, Battery connection wires is a special kind of steel that can effectively inhibit skin effect, therefore, the conductor resistance can be so small that to be ignored; because of parallel connection manner, the inductance between the connecting wire is still relatively large, and the external inductance L'' of the conductor is far larger than the internal inductance L', for what the inductance of the connecting
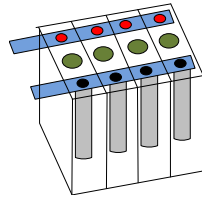
Fig. 10: Four cells connected in parallel
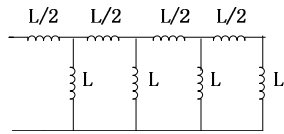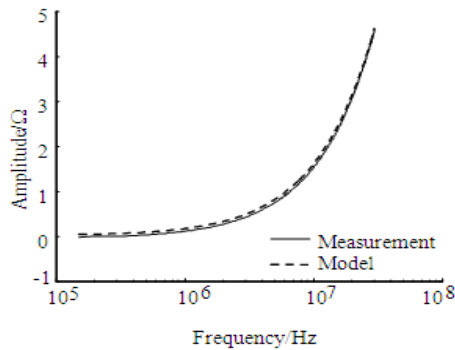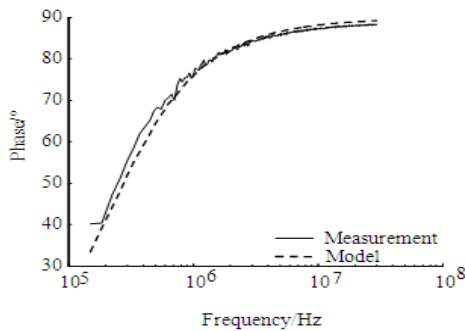

Fig. 11: Eequivalent inductance for cells in parallel

(a) amplitude-frequency

(b) phase-frequency

Fig. 12: Comparison of measured and simulated impedance curves for cells in parallel

wire cannot be ignored. the length of connecting steel between each of the two battery cells is with half of the electrode, combining with the method of calculation of the conductor inductance, inductance value of the connecting wire is 1/2 of the pair of electrodes, the equivalent inductance series-parallel circuit diagram in Fig. 11:

$$L_{parallel} = \frac{171}{170}L \approx L \qquad (14)$$

The model parameters of battery in parallel:

$$R_{parallel} = \frac{1}{4} \times (R_0 + R_{ac}(f)) + k_3$$

where $k_3 = 0.03$ is correction factor for the inductance value of batteries in parallel. Figure 12 shows the comparison of the measured impedance curve and the calculated impedance curve.

Since the steel connected between the cells will affect the overall impedance of the battery pack, and also the series-parallel connection of the batteries may causes the parasitic capacitance between the electrodes and the parasitic inductance on the connecting steel, there is a certain error between the model calculated values and the actual measured values.

CONCLUSION

A method to establish the high frequency circuit model of the battery based on its impedance characteristics and the structure of battery cell is present in this study. The high-frequency circuit model of battery are developed including instructions for calculating the model's parameter. The high-frequency models of cell, cells connected in series, cells connected in parallel are validated by the measurement in the frequency range from 150 kHz to 30 MHz. the measured impedance value of the battery and the calculated impedance value were compared to analyze the causes of the error. The results allow the prediction of the conducted behavior of the battery including the high frequency losses where batteries mainly react as an inductance with a comparatively high impedance, also it allows to predict the effect of batteries as spreading path for EMI and the external electric fields and magnetic fields generated by the batteries.

ACKNOWLEDGMENT

REFERENCES

Aesic, K. and Q.A. Wei, 2011. Hybrid battery model capable of capturing dynamic circuit characteristics and nonlinear capacity effects. IEEE T. Energy Conver., 26(12): 1172-1180.

Chen, M., A. Gabriel and M. Rincon, 2006. accurate electrical battery model capable of predicting runtime and I-V performance. IEEE T. Energy Conver., 21(7): 504-511.

Ehsani, M., G. Yimin and J.M. Miller, 2007. Hybrid electric vehicles: architecture and motor drives. Proc. IEEE, 95(4): 719-728.

Madi, A., J.L. Young and K. Rajashekara, 2008. Power electronics and motor drives in electric, hybrid electric and plug-in hybrid electric vehicler. IEEE T. Ind. Electron., 55(6): 2237-2245.

Mutoh, N., M. Nakanishi, M. Kanesaki and J. Nakashima, 2005. EMI noise control methods suitable for electrical vehicles drive systems. IEEE T. Electromagn. C., 47(12): 930-937.

Omar, H., V.M. Joeri and L.A. Philippel, 2012. Modeling and implementation of a multidevice interleaved DC/DC converter for fuel cell hybrid electric vehicle. IEEE T. Power Electr., 27(11): 4445-4458.

Zhang, J., S.C. Sharif and M. Alahmad, 2010. Modeling discharge behavior of multicell battery. IEEE T. Energy Conver., 25(12): 1133-1141.